Available online at www.sciencedirect.com
SCIENCE DIRECT®
Journal of Chromatography A, 1038 (2004) 275–282
JOURNAL OF CHROMATOGRAPHY A
www.elsevier.com/locate/chroma

# Determination of aggregation thresholds of UV absorbing anionic surfactants by frontal analysis continuous capillary electrophoresis☆

Thomas Le Saux, Anne Varenne, Pierre Gareil*

*Laboratoire d'Electrochimie et Chimie Analytique, Ecole Nationale Supérieure de Chimie de Paris, UMR CNRS 7575, 11 Rue Pierre et Marie Curie, F-75231 Paris Cedex 5, France*

Received 15 July 2003; accepted 22 January 2004

Available online 14 April 2004

**Abstract**

Aggregation of anionic surfactants was investigated by frontal analysis continuous capillary electrophoresis (FACCE), a method involving the continuous electrokinetic introduction of the surfactant sample into the separation capillary. This process results in a partial separation of the monomeric and aggregated forms without perturbing the monomer-aggregate equilibrium. The critical micelle concentration (CMC) can then be easily derived from the height of the firstly detected migration front, corresponding to the monomeric form. This approach is exemplified with octyl and dodecylbenzenesulfonates and compared with conductimetry and surface tension measurements. FACCE turns out to be an effective method for the determination of CMC and intermediate aggregation phenomena with very small sample and short time requirements.


*Keywords:* Frontal analysis continuous capillary electrophoresis; Critical micellar concentration; Aggregation thresholds; Surfactants

## 1. Introduction

Surfactants have amphiphilic properties resulting from their unique structure that is made up of a hydrophobic hydrocarbonaceous tail comprising at least six–eight carbon atoms, and of a hydrophilic, more or less bulky, neutral or ionic head. When their concentration in solution is over a threshold value, they form aggregates, with the part of solvent-like polarity turned outside, facing the solvent. The first type of aggregates appearing beyond this threshold concentration can be often considered spherical in shape and is called micelles [1]. For still higher surfactant concentrations, more complex aggregate structures of oblate or prolate forms can appear, built up of either a single surfactant layer or of a surfactant bilayer, as is the case in vesicles. In aqueous media at a macroscopic level, the aggregated particles behave as pseudo-phases which have found widespread industrial applications in aqueous media for the solubilization of hydrophobic compounds, e.g. in the pharmaceutical, healthcare, painting, detergence or environment depollution areas [2]. More recently, surfactants have also aroused a great interest in chemical synthesis and analytical chemistry. The concentration threshold corresponding to the onset of micelle formation, or critical micelle concentration (CMC), strongly depends on the surfactant nature but also on temperature and on the medium (solvent composition, pH, ionic strength, counter-ion, in case of an ionic surfactant) [3–5]. As a consequence of this, CMC values may depend on the surfactant purity and the medium conditions can be tailored to adjust aggregation thresholds. Furthermore, surfactants are often produced as homologue mixtures and also utilized in real life applications in more or less complex formulations, which may widely affect their aggregation properties. For the optimization of the formulations and processes in all of these areas, the knowledge of CMC or aggregation concentration data is therefore of prime importance. A number of analytical techniques have been commonly implemented to obtain these data, among which conductimetry [6], potentiometry [7], surface tension measurement [8], absorbance and fluorescence spectroscopy [9], light scattering [10], cyclic voltammetry [11] and NMR [12]. The choice of

☆ Presented at the 27th International Symposium on High-Performance Liquid-Phase Separations and Related Techniques, Nice, 15–19 June 2003.

* Corresponding author. Tel.: +33-1-55426371; fax: +33-1-44276750.
*E-mail address:* pierre-gareil@enscp.jussieu.fr (P. Gareil).

0021-9673/$ – see front matter © 2004 Elsevier B.V. All rights reserved.
doi:10.1016/j.chroma.2004.03.006

a technique may depend on its availability, easiness of use, but also on the surfactant nature (ionic and non-ionic) and its spectroscopic properties. More recently, capillary zone electrophoresis has also been established for the determination of CMC values of UV-transparent, anionic and cationic surfactants with low sample consumption [13–18]. The method described consists in determining the surfactant concentration in the operating electrolyte inducing a sudden variation of the apparent mobility of an appropriate marker interacting with the surfactant. It requires, however, a fast kinetics of interaction between the surfactant and the marker. Furthermore, the capillary electrophoresis instrumentation has been employed to determine the CMC values of ionic surfactants from the variation of the current intensity in terms of the total surfactant concentration inside the capillary, in an analogous way to conductimetry [19].

The purpose of this work was to develop an alternative capillary electrophoretic method for the determination of CMC values, applying the principles of frontal analysis continuous capillary electrophoresis (FACCE). The interest of this method, reminiscent of moving boundary electrophoresis, was emphasized by Gao et al. [20] a few years ago, for the determination of binding constants between two macromolecular partners. The method consists in continuously, electrokinetically introducing the sample solution into the separation capillary. Under such conditions, the chemical equilibrium between the free and associated forms is not perturbed as only a partial separation takes place. The resulting migration front of the free form is then usually exploited to yield the concentration of both forms and hence interaction parameters through mass balance equations. Following our previous determinations of the binding parameters pertaining to binary systems of biological interest by FACCE [21,22], we investigated in this work the auto-associative systems of anionic surfactants. Octyl and dodecylbenzenesulfonates were selected as model molecules for the assessment of this method, to allow easy direct absorbance monitoring.

## 2. Materials and methods

### 2.1. Surfactants and reagents

The studied surfactants, sodium octylbenzenesulfonate ($C_8$), sodium dodecylbenzenesulfonate ($C_{12}$) and benzyl alcohol (99% purity) were purchased from Aldrich (Saint-Quentin-Fallavier, France). Sodium tetraborate, and formamide (both 99% purity) were from Fluka (Saint-Quentin-Fallavier, France) and potassium chloride from Merck (Darmstadt, Germany). Water used throughout was produced by an Alpha Q system (Millipore, Molsheim, France).

### 2.2. Capillary electrophoresis

Electrophoretic measurements were performed with a HP$^{3D}$CE (Agilent Technologies, Waldbronn, Germany) capillary electrophoresis system. This apparatus automatically realizes all the steps of the analytical protocols, including capillary conditioning, sample introduction, voltage application and diode array detection and allows to run unattended method sequences. Data were handled by the HP Chemstation software and Microsoft Excel. The separation capillaries (Phymep, Paris, France) were of bare fused silica, 35 cm (26.5 cm to the detector) × 50 μm i.d. The background electrolyte (BGE) was a 20 mM sodium borate buffer, pH 9.2 (ionic strength: 10 mM). The running voltage was 10 kV. The temperature of the capillary cartridge was set at 30 °C. The sample tray was also maintained at 30 °C by an external water bath. Analytes were detected by UV absorbance at 200, 222 or 230 nm, according to cases. Benzyl alcohol (0.01% (v/v), in the BGE) or formamide (0.001% (v/v), in the BGE) were used as neutral markers to determine the electroosmotic mobility. For zone electrophoresis experiments, samples were introduced hydrodynamically by applying a 30 mbar pressure for 2 s (approximately, 3 nl) to the neutral marker, BGE and sample vials, successively. For frontal analysis experiments, the neutral marker, BGE and surfactant sample were first hydrodynamically introduced under 30 mbar for 2 s (approximately, 3 nl each). Next, a continuous electrokinetic introduction of the surfactant sample under the separation voltage was performed. The sample solutions were prepared from 20 mM $C_8$ and 0.2 M $C_{12}$ parent solutions in the 20 mM borate buffer used as BGE. These solutions were next diluted with the same buffer to generate appropriate series of surfactant solutions of known concentrations. New capillaries were conditioned by successive flushes with 1 M NaOH, 0.1 M NaOH, water and finally equilibrated with the separation electrolyte, each under 935 mbar for 10 min (about 40 capillary volumes). Between runs, the capillaries were washed with 0.1 M NaOH for 3 min, water for 2 min and BGE for 5 min. Capillaries were rinsed with water and dried by air when not in use.

### 2.3. Conductimetry

Specific conductivities were measured at 30 °C using a Radiometer Analytical CDM210 conductimeter (Villeurbanne, France) equipped with a XE100 cell. Prior to each series of measurements, the apparatus was calibrated with a 0.1 M KCl solution at 30 °C. The $C_8$ and $C_{12}$ surfactant solutions used for conductivity measurements were in the 0–20 mM concentration range in the 20 mM borate buffer.

### 2.4. Surface tension measurements

The surface tension measurements were carried out at 30 °C using a KS210ST apparatus from Krüss (Palaiseau, France) equipped with a platinum blade. The surfactant solutions used for these measurements were the same as those used for conductimetry.

## 3. Results and discussion

### 3.1. Capillary zone electrophoresis of free surfactants

Capillary zone electrophoresis was first implemented in a classical 20 mM sodium borate buffer to characterize the purity of the surfactant samples. A short plug of neutral marker (benzyl alcohol) was also injected to allow calculation of the electrophoretic mobilities. The injection protocol was designed to avoid contact between the neutral marker and surfactants. Fig. 1 shows the electropherograms obtained for the $C_8$ and $C_{12}$ surfactant samples. Whereas the $C_8$ sample was devoid of noticeable impurities, the $C_{12}$ sample presumably contained minor amounts of surfactant homologues. Spiking the $C_{12}$ solution with the $C_8$ one allowed us to tentatively assign the impurity peaks to alkylbenzenesulfonates having even numbered carbon atom alkyl chains from $C_2$ to $C_{10}$. Assuming identical molar extinction coefficients led to a purity for the $C_{12}$ surfactant sample of ca. 84% (Table 1), but this value is likely under-estimated as the molar extinction coefficients of the shorter alkyl chain length surfactants should be markedly higher. The electrophoretic mobilities evaluated from migration times at peak apex were $-25.1 \times 10^{-5}$ and $-22.6 \times 10^{-5}\,cm^2\,V^{-1}\,s^{-1}$ for the $C_8$ and $C_{12}$ surfactants, respectively (30 °C, 10 mM ionic strength). In spite of the lower sample concentrations used for this measurement (both 0.1 mM for the $C_8$ and $C_{12}$ samples, respectively),

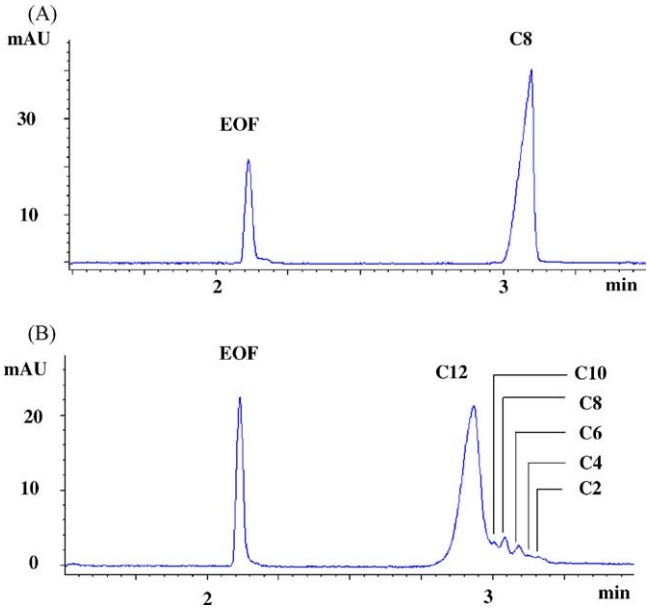


Fig. 1. Zone electropherograms of: (A) sodium octyl and (B) sodium dodecylbenzenesulfonate. Fused silica capillary, 35 cm (detection: 26.5 cm) × 50 μm i.d., BGE: 20 mM sodium borate buffer, pH 9.2 (ionic strength: 10 mM). Applied voltage: +10 kV (current intensity: 5 μA). Temperature: 30 °C. UV absorbance detection at 200 nm. Hydrodynamic injection of benzyl alcohol (30 mbar, 2 s), BGE (30 mbar, 2 s), surfactant sample (30 mbar, 2 s). EOF: electroosmotic flow. Peak assignment: $C_{12}$: dodecyl-; $C_8$: octyl-benzenesulfonate. Tentative peak assignment: $C_{10}$: decyl-; $C_6$: hexyl-; $C_4$: butyl-; $C_2$: ethyl-benzenesulfonate.

Table 1
Tentative qualitative and quantitative compositions of the commercial sodium dodecylbenzenesulfonate sample

| Migration times (min) | Peak assignment | Normalized peak area (%) |
|---|---|---|
| 2.93 | $C_{12}$ | 84 |
| 3.00 | $C_{10}$ | 3.5 |
| 3.04 | $C_8$ | 7 |
| 3.09 | $C_6$ | 2.5 |
| 3.12 | $C_4$ | 2 |
| 3.16 | $C_2$ | 1 |

Migration times and normalized peak areas corresponding to the electropherogram given in Fig. 1.

these values were likely slightly over-estimated due to some degree of peak fronting.

### 3.2. Characterization of aggregation phenomena by conventional methods

#### 3.2.1. Conductivity measurements

Conductivity measurements were performed for $C_8$ and $C_{12}$ alkylbenzenesulfonates at varying concentrations in a 20 mM borate buffer, for which the surfactants were either in free form or partially aggregated.

For the $C_8$ surfactant, the variation of the specific conductivity in terms of the surfactant concentration clearly presents two linear tendencies (Fig. 2A), on both sides of a concentration of 9.8 mM. This breakdown in the slope of the conductivity variation corresponds to the aggregation threshold of the surfactant, i.e., to the formation of surfactant micelles when the total surfactant concentration is >9.8 mM. The slower increase in conductivity after this point is mainly due to the sodium counter-ion condensation around the micelle, which contributes to decrease the free sodium ion concentration in the medium. Table 2 gives the parameters (slope and intercept) of the two regression straight lines obtained with their 95% confidence intervals. From these, the 95% confidence interval was derived for the CMC value determined as the abscissa of the intersection points of the most distant straight lines. This resulted in CMC values of $9.8 \pm 0.3$ and $9.8 \pm 0.4$ mM at 95 and 99% confidence, respectively.

The specific conductivities of $C_{12}$ surfactant samples were measured as a function of the concentration under the same conditions as for the $C_8$ one, but contrary to previously, no discontinuity in the curve derivative can be made apparent (Fig. 2B). Moreover, all the data points can be fitted to a single straight line with a high correlation coefficient. It is obviously not possible to determine the CMC value for the $C_{12}$ surfactant in this medium by this method. Nevertheless, it is worthy noting that all the experimental points corresponding to 0.3–2 and 13–20 mM concentrations are located below the regression straight line, whereas those obtained with 3–12 mM concentrations were systematically above the line. This behavior indicates that the data points did not randomly distribute apart the regression straight line and that in effect two different, but significantly

Table 2
Parameters (regression coefficients, slopes, intercepts) of the regression straight lines for the variation of the specific conductivity of sodium octylbenzenesulfonate in 20 mM sodium borate buffer, pH 9.2 (ionic strength, 10 mM) at 30 °C (Fig. 2A) and resulting CMC value obtained as the abscissa of their intersection point

| Surfactant concentration range (mM) | Regression coefficient ($R^2$) | Slope (mS cm$^{-1}$ mM$^{-1}$) | Intercept (mS cm$^{-1}$) | Intersection point (CMC value) (mM) |
|---|---|---|---|---|
| 1–9 | 0.9998 ($n = 9$) | 0.069 ± 0.001* | 0.863 ± 0.006* | 9.8 ± 0.3* |
| 11–20 | 0.9988 ($n = 10$) | 0.029 ± 0.001* | 1.259 ± 0.017* | |

* 95% confidence interval.

undiscernible tendencies were likely to occur. This only led us to postulate that the CMC value was near to 2 mM.

### 3.2.2. Surface tension measurements

In order to confirm the results obtained by conductimetry, the surfactant solutions were also submitted to surface tension measurements. The variations of the surface tension of the $C_8$ and $C_{12}$ surfactant samples as a function of their total concentrations in a 20 mM sodium borate buffer are shown in Fig. 3. For the $C_8$ surfactant, the experimental curve exhibits a more pronounced decline starting at a concentration of ca. 3 mM and next goes past a minimum at about 7.5 mM. The surface tension then becomes almost constant for concentrations in excess of ca. 10 mM. These measurements confirm the transition from the surfactant monomer form to a monomer–micelle equilibrium over this range of concentration. The depressed shape of the curve in this range may be explained by the presence of impurities in the sample solutions. The great sensitivity of surface tension to the purity of the sample solution likely precludes this method from yielding a precise and reliable CMC value for this surfactant.

Unsurprisingly, the curve showing the variation of the surface tension for the $C_{12}$ surfactant sample as a function of its concentration was even more difficult to interpret. As discussed before, the $C_{12}$ surfactant sample was not as pure as the $C_8$ one and probably contained homologue compounds. It can be emphasized, nevertheless, that the surface tension of this sample reached a plateau value for concentration over ca. 2 mM, in accordance with conductimetric measurements. In spite of this, surface tension measurements do not appear to be a convenient technique for the determination of aggregation thresholds, especially when the samples to be studied is not of high purity.

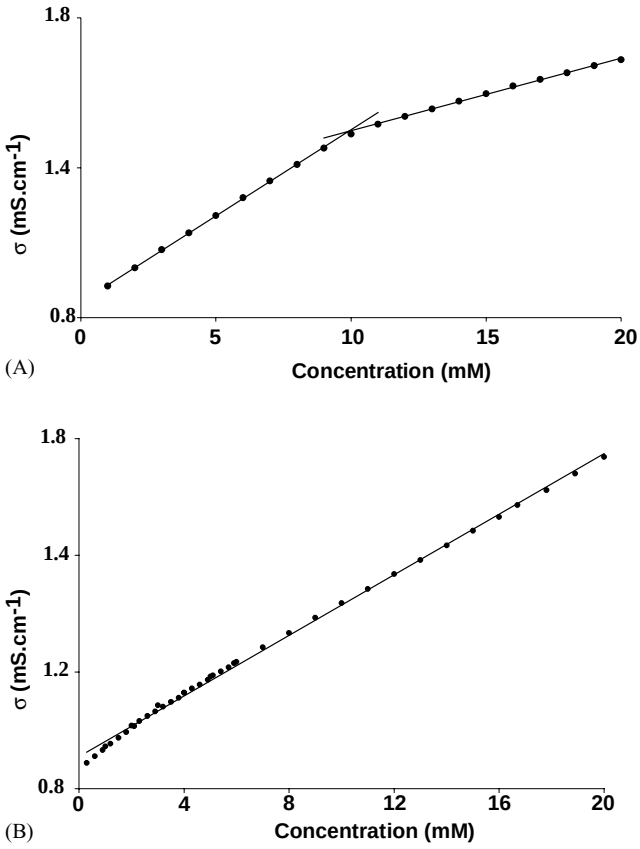


Fig. 2. Variation of the specific conductivity $\sigma$ of: (A) sodium octyl- and (B) sodium dodecyl-benzenesulfonate solutions as a function of their concentration in a 20 mM sodium borate buffer, pH 9.2. Temperature: 30 °C. The solid lines represent the least squares regression straight lines: A, see Table 2; B, $y = 0.0519x + 0.9102$ ($R^2 = 0.998$, $n = 41$).

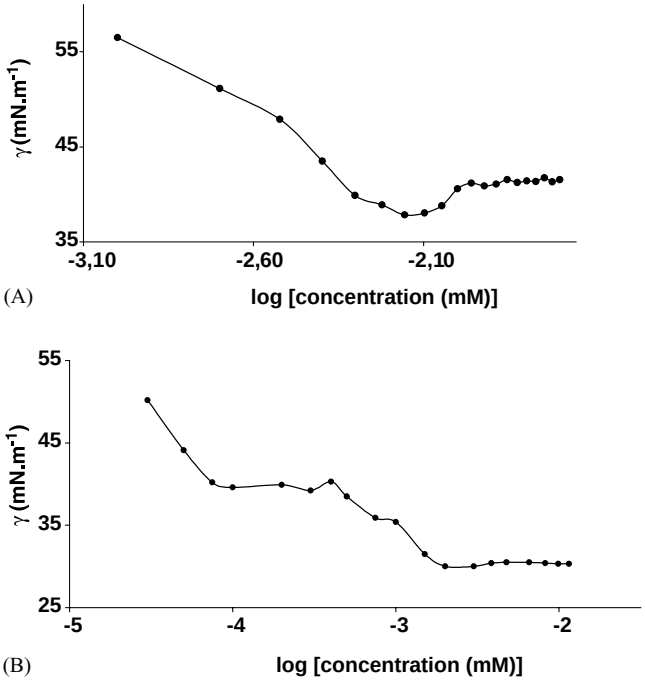


Fig. 3. Variation of the surface tension $\gamma$ of: (A) sodium octyl- and (B) sodium dodecyl-benzenesulfonate solutions as a function of their concentration in a 20 mM sodium borate buffer, pH 9.2. Temperature: 30 °C.

### 3.3. Frontal analysis of free and aggregated surfactants

Frontal analysis continuous capillary electrophoresis was next investigated as a new approach to access to aggregation thresholds of surfactant solutions. In this prospect, the separation capillary was first filled with the medium retained throughout this study (20 mM sodium borate buffer, pH 9.2). Surfactant solutions prepared in the same buffer were then continuously introduced into the capillary in the electrokinetic mode, applying 10 kV. In order to ensure a better continuity between the plain buffer and the surfactant zone, this electrokinetic injection was preceded by the hydrodynamic introduction of a short plug of the same solution. Still before this step, a short plug of neutral marker solution was also hydrodynamically injected to standardize the frontal electropherograms in terms of electrophoretic mobilities.

#### 3.3.1. Octylbenzenesulfonate

Fig. 4 shows a series of frontal electropherograms obtained with $C_8$ surfactant solutions of varying concentrations (7–13 mM), encompassing the CMC value. As expected, the migration fronts relevant to the anionic surfactant were detected after the neutral marker peak. Depending on the initial concentration of the sample, a single or several migration fronts were observed. For concentrations <9 mM, migration fronts F1 and F3 were detected. From 10 mM upwards, the electropherograms exhibited an additional front, F2, located between F1 and F3. The presence of these fronts is representative of the different free and aggregated forms existing in the sample solution. In order to assign these fronts, the electrophoretic mobilities were measured at the inflection point of all migration fronts, since they should correspond to the

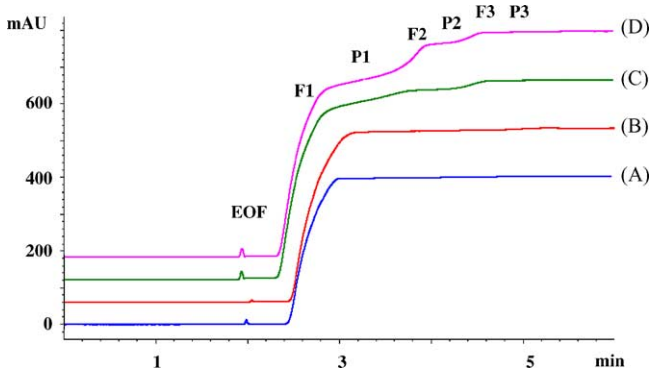


Fig. 4. Frontal analysis continuous capillary electophoresis of sodium octylbenzenesulfonate at various concentrations: (A) 7 mM, (B) 9 mM, (C) 11 mM and (D) 13 mM. Fused silica capillary, 35 cm (detection: 26.5 cm) × 50 μm i.d. BGE: 20 mM sodium borate buffer, pH 9.2 (ionic strength: 10 mM). Applied voltage: +10 kV (initial current intensity: 5 μA). Temperature: 30 °C. UV absorbance detection at 200 nm. Sample: $C_8$ surfactant at the specified concentration in the BGE. Injection: benzyl alcohol (30 mbar, 2 s), BGE (30 mbar, 2 s), sample (30 mbar, 2 s), followed by a continuous electrokinetic sample introduction under 10 kV. EOF: electroosmotic flow. F1, F2, F3: migration fronts of monomeric, micellar and oligomeric forms, respectively. P1, P2 and P3: corresponding concentration plateaus.

mobilities measured at peak apex in zone electrophoresis for the various surfactant forms. The measured values, however, turned out to decrease (in absolute value) on increasing the surfactant concentration in the sample, as reported below: from $-21.0 \times 10^{-5}$ to $-13,7 \times 10^{-5}$ $cm^2\,V^{-1}\,s^{-1}$ for front F1, $-38.2 \times 10^{-5}$ to $-35.1 \times 10^{-5}$ $cm^2\,V^{-1}\,s^{-1}$ for front F2 and $-46.7 \times 10^{-5}$ to $-41.5 \times 10^{-5}$ $cm^2\,V^{-1}\,s^{-1}$ for front F3. This complex behavior could be due to: (i) an electroosmotic mobility mismatch between the section of the capillary filled with the buffer and that containing the surfactant; (ii) a viscosity increase in the capillary section containing the surfactant; or (iii) a decrease in electric field in this latter section, as compared to the field created in the plain buffer section. Nevertheless, the migration time of the neutral marker hydrodynamically injected just before the continuous sampling of the surfactant did not reveal any significant increase of the mean electroosmotic mobility (average value: $76 \times 10^{-5}$ $cm^2\,V^{-1}\,s^{-1}$), which might result from some adsorption of the anionic surfactant to the capillary wall. To better appreciate any variation in the electroosmotic flow occurring after the detection of benzyl alcohol in the preceding experiments, an additional series of electroosmotic measurements was also performed for each surfactant solution totally filling the capillary, by injecting a small volume (ca. 3 nl) of formamide. The results showed that the electroosmotic mobility in this medium slightly decreased upon increasing surfactant concentration, as governed by the concurrent increase in the thickness of the electric double layer. Using the CE instrument and applying a method already described [23], the viscosities of the surfactant solutions were next determined as a function of their concentration, showing a slight decrease in viscosity upon increasing concentration. So, both electroosmosis and viscosity effects failed to explain the apparent decrease in electrophoretic mobility at the inflection point of the migration fronts, as surfactant concentration increases. This behavior should then mainly result from decreasing electric fields in the capillary section occupied by the surfactant, induced by the increasing conductivities of surfactant solutions. The net effect was a faster apparent migration of the surfactant fronts, carried over by the electroosmotic flow in the direction opposite to migration. In spite of this apparent variation in the electrophoretic mobilities corresponding to the migration fronts, front F1, observed whatever the $C_8$ surfactant concentration, can be assigned to the free surfactant form. The electrophoretic mobility at the inflection point of this front was all the closer to the $C_8$ surfactant mobility observed in zone electrophoresis than the $C_8$ surfactant concentration was lower. Front F2, detected above a certain concentration threshold, and migrating ahead of the free form counter-electroosmotically, can be assigned to the micellar form of the $C_8$ surfactant. The presence of a third migration front, F3, at all the concentrations experienced, for an electrophoretic mobility of the order of twice that of the free surfactant, suggests the existence of intermediate aggregated forms, possibly dimers. Fig. 5A shows that the

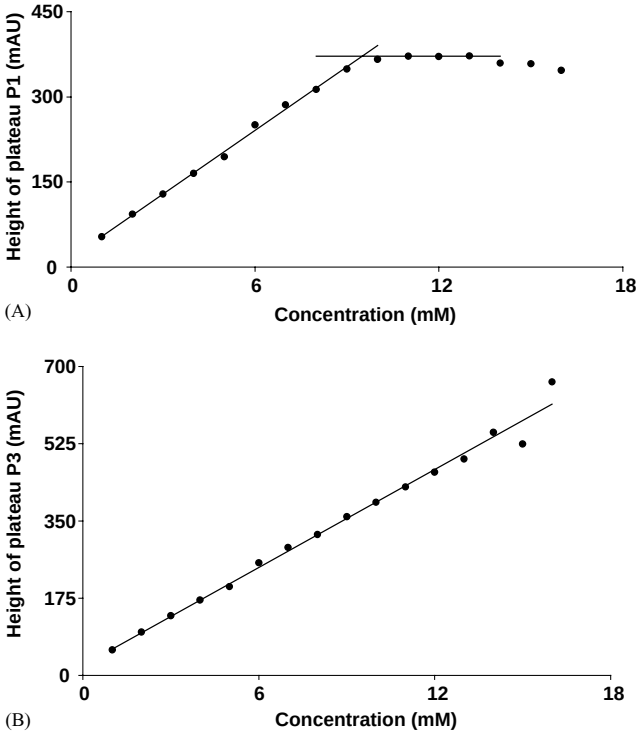


Fig. 5. Variation of the heights of the concentration plateaus: (A) P1 (measured at a constant electrophoretic mobility of $-31 \times 10^{-5}$ cm$^2$·V$^{-1}$·s$^{-1}$) and (B) P3 (measured at a constant electrophoretic mobility of $-51 \times 10^{-5}$ cm$^2$·V$^{-1}$·s$^{-1}$) shown in Fig. 4 as a function of the total $C_8$ surfactant concentration. Experimental conditions as for Fig. 4, except detection wavelength, 230 nm. The solid lines represent the least squares regression straight lines: A, see Table 3; B, $y = 36.97x + 23.00$ ($R^2 = 0.988$, $n = 16$).

height of the first concentration plateau, P1, which corresponds to the free form concentration, varied linearly with the total $C_8$ surfactant concentration, before leveling off for concentrations higher than about 10 mM. The height of concentration plateau P3, which corresponds to all surfactant forms in equilibrium and locally present, was also proportional to the total surfactant concentration (Fig. 5B), which demonstrated both the linearity of the detector response over this range of absorbance and the similarity of the extinction coefficients of the various surfactant forms. Thus, the step observed in Fig. 5A for the variation of the free form concentration should correspond to the CMC value being reached. Table 3 shows that the CMC value, determined as the abscissa of the intersection point of the two linear tendencies observed, is in full agreement with the values previously obtained from conventional methods. Furthermore, it is worthy of note that the free concentration at plateau P1 tends to decrease for total surfactant concentrations above 13 mM (Fig. 5A). This tendency should account for the expected CMC decrease for ionic surfactants on increasing ionic strength of the medium [14]. Finally, it was also observed that the height of concentration plateau P3 exhibited its most pronounced increase for surfactant concentrations close to the CMC value, suggesting a favored formation of intermediate aggregates in this domain.

In addition to this, the previous series of experiments was also exploited to obtain an independent evaluation of the CMC value according to the method described by Cifuentes et al. [19]. For this prospect, the current intensity was measured for each surfactant concentration at a time for which the capillary is filled up with the surfactant solution. The plot of the current intensity versus the total $C_8$ surfactant concentration (not shown) displays two linear tendencies, the regression parameters of which are reported in Table 4. This method yields a CMC value of 9.5 mM with a 95% confidence interval overlapping those obtained before.

### 3.3.2. Commercial sample of dodecylbenzenesulfonate

The same experimental protocol for frontal analysis continuous capillary electrophoresis was resumed to investigate the behavior of a less pure $C_{12}$ surfactant sample. Fig. 6 shows that the number of migration fronts detected is dependent on the total concentration of the surfactant. For total $C_{12}$ surfactant concentrations lower than 0.5 mM, solely front F1 was observed, the mobility of which at inflection point was decreasing in absolute value ($-20.1 \times 10^{-5}$ to $-17.6 \cdot 10^{-5}$ cm$^2$ V$^{-1}$ s$^{-1}$) on increasing concentration. The comparison of theses values with those determined before in zone electrophoresis for the $C_{12}$ surfactant sample lend support to assigning front F1 to the monomeric form of the surfactant. From 0.5 mM concentrations, front F2 was detected with measured mobilities at inflection point between $-46.0 \times 10^{-5}$ and $-44.0 \times 10^{-5}$ cm$^2$ V$^{-1}$ s$^{-1}$, according to the concentration. This migration front should correspond to the micellar form of the $C_{12}$ surfactant. For total sample concentrations above 3 mM, a third migration front, F3, became apparent (mobilities at inflection point varying between $-47.4 \times 10^{-5}$ and $-46.8 \times 10^{-5}$ cm$^2$ V$^{-1}$ s$^{-1}$

Table 3
Parameters (regression coefficients, slopes, intercepts) of the regression straight lines for the variation of the absorbance on concentration plateau P1 as a function of the total concentration of sodium octylbenzenesulfonate (plot shown in Fig. 5A)

| Surfactant concentration range (mM) | Regression coefficient ($R^2$) | Slope (AU mM$^{-1}$) | Intercept (AU) | Intersection point (CMC value) (mM) |
|---|---|---|---|---|
| 1–9 | 0.997 ($n = 9$) | 37.4 ± 1.9* | 17 ± 10* | 9.5 ± 0.8* |
| 11–13 | | 0 | 371.6 ±1.5* (mean value $n = 3$) | |

Experimental conditions (see Fig. 4), except for the wavelength, 230 nm. The CMC value was obtained as the abscissa of the intersection point.
* 95% confidence interval.

Table 4
Parameters (regression coefficients, slopes, intercepts) of the regression straight lines for the variation of the current intensity across the electrophoretic capillary as a function of the concentration of sodium octylbenzenesulfonate in 20 mM sodium borate buffer, pH 9.2 (ionic strength: 10 mM) at 30 °C and resulting CMC value obtained as the abscissa of their intersection point

| Surfactant concentration range (mM) | Regression coeffficient ($R^2$) | Slope ($\mu A\,mM^{-1}$) | Intercept ($\mu A$) | Intersection point (CMC value) (mM) |
|---|---|---|---|---|
| 1–9 | 0.997 ($n = 9$) | 0.40 ± 0.02* | 5.9 ± 0.1* | 9.5 ± 0.6* |
| 10–14 | 0.996 ($n = 5$) | 0.18 ± 0.02* | 8.0 ± 0.3* | |

35 cm × 50 μm i.d. capillary, applied voltage: +10 kV.
* 95% confidence interval.

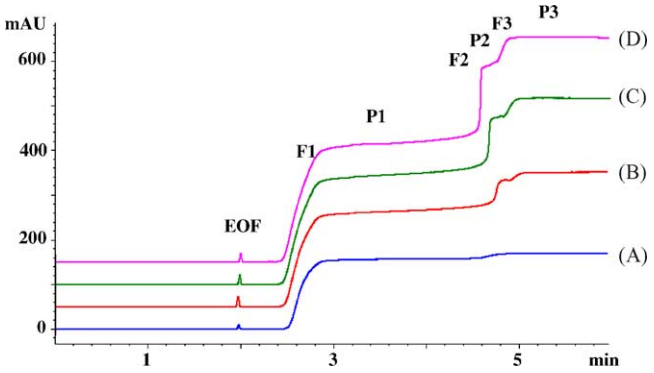


Fig. 6. Frontal analysis continuous capillary electrophoresis of a commercial sample of sodium dodecylbenzenesulfonate at various concentrations: (A) 2 mM, (B) 4 mM, (C) 6 mM and (D) 8 mM. Experimental conditions as in Fig. 4, except for the sample. EOF: electroosmotic flow (formamide peak). F1, F2, F3: migration fronts of monomeric, micellar and mixed aggregate forms, respectively. P1, P2 and P3: corresponding concentration plateaus.

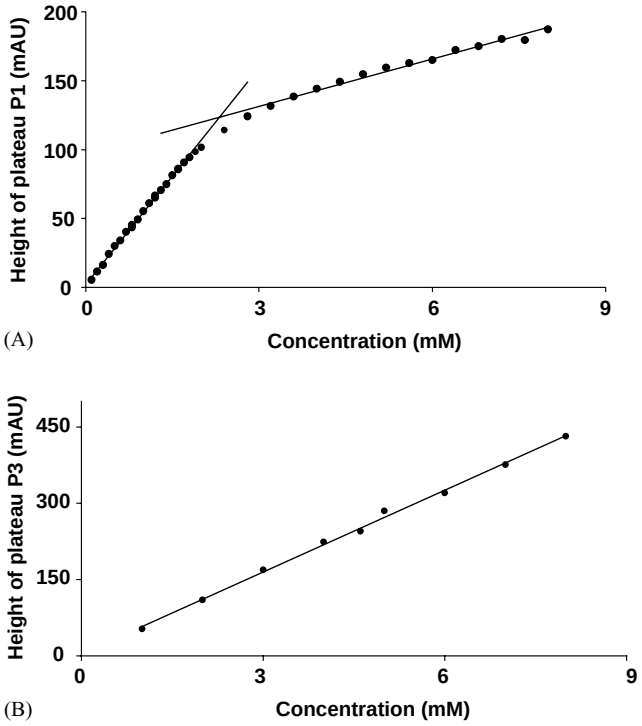


Fig. 7. Variation of the heights of concentration plateaus: (A) P1 (measured at a constant electrophoretic mobility of $-37 \times 10^{-5}\,cm^2 \cdot V^{-1} \cdot s^{-1}$) and (B) P3 (measured at a constant electrophoretic mobility of $-51 \times 10^{-5}\,cm^2 \cdot V^{-1} \cdot s^{-1}$) shown in Fig. 6 as a function of the total $C_{12}$ surfactant concentration. Experimental conditions as for Fig. 6, except for the detection wavelength, 222 nm. The solid lines represent the least squares regression straight lines: A, see Table 4; B, $y = 53.51x + 4.40$ ($R^2 = 0.997$, $n = 9$).

according to the concentration), which might represent the breakthrough of mixed aggregates including shorter surfactant homologues.

Fig. 7A displays the variation of the height of plateau P1 following migration front F1 attributed to the monomeric form in terms of the total surfactant concentration, while Fig. 7B enables us to check the good linearity of the detector response within the range of concentrations studied. Conversely to what was established for the $C_8$ surfactant, Fig. 7A does nor exhibit a flat step, but solely a break in the slopes between two linear tendencies, apart from a $C_{12}$ concentration of 2.3 mM (Table 5). This peculiar behavior should correspond to the fact that, beyond the threshold of the $C_{12}$ surfactant micellization, shorter surfactant homologues contained in the commercial $C_{12}$ surfactant sample still remain free and migrate at the speed of front F1. It then seems likely that for higher total concentration of the $C_{12}$ sample, these impurities will be incorporated into the micelles to form mixed aggregates.

Table 5
Parameters (regression coefficients, slopes, intercepts) of the regression straight lines for the variation of the absorbance on concentration plateau P1 as a function of the total concentration of the commercial sample of sodium dodecylbenzenesulfonate (plot shown in Fig. 7A)

| Surfactant concentration range (mM) | Regression coeffficient ($R^2$) | Slope ($AU\,mM^{-1}$) | Intercept (AU) | Intersection point (CMC value) (mM) |
|---|---|---|---|---|
| 0.1–2 | 0.998 ($n = 21$) | 52.4 ± 1.1* | 2.2 ± 1.6* | 2.30 ± 0.09* |
| 2.7–8 | 0.984 ($n = 14$) | 11.5 ± 0.9* | 97 ± 5* | |

Experimental conditions (see Fig. 6), except for the wavelength, 222 nm. The CMC value was obtained as the abscissa of the intersection point.
* 95% confidence interval.

*3.3.3. Fast determination of the aggregation threshold of a UV absorbing, anionic surfactant*

The preceding results demonstrate that only four concentration levels can be enough for a reliable determination of the aggregation threshold of a pure, UV absorbing, anionic surfactant. In fact, assuming a linear detector response, a single frontal analysis continuous capillary electrophoresis performed for a known surfactant concentration above the aggregation threshold allows to obtain a first estimation of the aggregation threshold by normalizing the height of the concentration plateau of the free surfactant (so called P1) to that of the surfactant aggregate in equilibrium with its free form (so called P3). A more precise determination can next be obtained by realizing three additional experiments with surfactant samples at known concentrations below the aggregation threshold. The measured heights of the concentration plateaus then allow to check detector linearity and to plot a calibration straight line. It should be emphasized that the same experiments can be exploited to obtain an additional and independent evaluation of the aggregation threshold using the current intensity data, in a way equivalent to conductivity measurements. In case of a mixture of surfactants, the frontal method gives access to the aggregation threshold of the more aggregative surfactant (i.e. the one having the longer hydrophobic tail), if its content is known.

## 4. Conclusion

This work demonstrates the suitability of frontal analysis continuous capillary electrophoresis for the determination of the critical micellar concentrations or aggregation thresholds of UV absorbing, anionic surfactants. Especially, it allows to detect the formation of intermediate, oligomeric aggregates. In case of mixtures of homologues, the method still allows to obtain the CMC of the one having the longest chain. Thus, this new method compares very favorably to conventional existing ones (conductimetry and surface tension measurements), as regards to its sensitivity to detect aggregation phenomena, precision of determination, speed, easiness of implementation and especially sample amount requirement. Especially, it does neither imply a fast equilibrium between surfactant monomers and aggregates, nor between the surfactant and any molecular marker, as is the case in capillary zone electrophoresis. Work is in progress in our group to extend the method to non-absorbing anionic, cationic and even to non-absorbing neutral surfactants.

## References

[1] E. Pramauro, E. Pelizzetti, Surfactants in Analytical Chemistry, Elsevier, Amsterdam, 1996.
[2] D.O. Shah, Micelles, Microemulsions and Monolayers, Sciences and Technology, Marcel Dekker, New York, 1998.
[3] D. Myers, Surfactant Science and Technology, VCH, New York, 1998.
[4] B.C. Paul, S.S. Islam, K. Ismail, J. Phys. Chem. B 102 (1998) 7807.
[5] E.S. Ahuja, J.P. Foley, Anal. Chem. 67 (1995) 2315.
[6] P.R. Martin, G. Prieto, C. Rega, L.M. Varela, F. Sarmiento, V. Mosquera, Langmuir 14 (1998) 4422.
[7] T. Nakashima, T. Anno, H. Kanda, Y. Sato, T. Kuroi, H. Fujii, S. Nagadome, G. Sugihara, Colloids Surf. B: Biointerfaces 24 (2002) 103.
[8] M.I. Gjerde, W. Nerdal, H. Hoiland, J. Colloid Interface Sci. 197 (1998) 191.
[9] H. Nakamura, A. Sano, K. Matsuura, Anal. Sci. 14 (1998) 379.
[10] E.D. Goddard, Colloids Surf. 19 (1986) 255.
[11] A.B. Mandal, B.U. Nair, J. Phys. Chem. 95 (1991) 9008.
[12] T.S. Lee, K.W. Woo, J. Colloid Interface Sci. 169 (1995) 34.
[13] J.C. Jacquier, P.L. Desbène, J. Chromatogr. A 718 (1995) 167.
[14] J.C. Jacquier, P.L. Desbène, J. Chromatogr. A 743 (1996) 307.
[15] C.-E. Lin, M.-J. Chen, H.-C. Huang, H.-W. Chen, J. Chromatogr. A 924 (2001) 83.
[16] C.-E. Lin, K.S. Lin, J. Chromatogr. A 868 (2000) 313.
[17] C.-E. Lin, T.Z. Wang, T.C. Chiu, C.C. Hsueh, J. High Resolution Chromatogr. 22 (1999) 265.
[18] Y. Mrestani, R. Neubert, H.H. Rüttinger, J. Chromatogr. A 868 (2000) 317.
[19] A. Cifuentes, J.L. Bernal, J.C. Diez-Masa, Anal. Chem. 69 (1997) 4271.
[20] J. Gao, P.L. Dubin, B. Muhoberac, Anal. Chem. 69 (1997) 2945.
[21] I. Porcar, H. Cottet, P. Gareil, C. Tribet, Macromolecules 32 (1999) 3922.
[22] I. Porcar, P. Gareil, C. Tribet, J. Phys. Chem. B 102 (1998) 7906.
[23] M.S. Bello, R. Rezzonico, P.G. Righetti, J. Chromatogr. A 659 (1994) 199.